

11. DATA PROCESSING

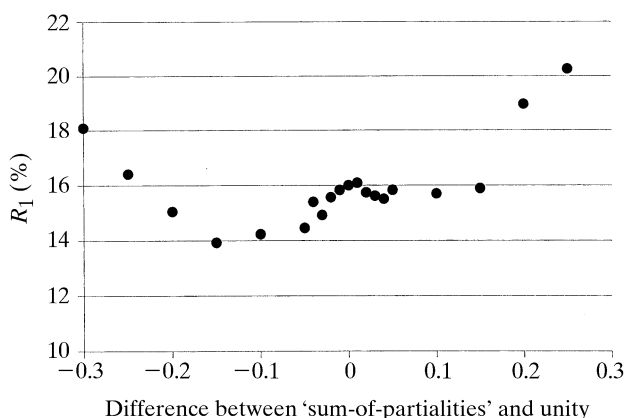


Fig. 11.5.7.4.  $R$  factor as a function of the difference of calculated 'sum-of-partialities' and unity for the estimates of full reflections when method 1 is used for the scaling and averaging of a  $\varphi$ X174 data set (Dokland *et al.*, 1997).

11.5.7.3. Statistics for rejecting reflections and data quality as a function of frame number

The behaviour of the  $R$  factor *versus* frame number (Fig. 11.5.7.5) is more monotonic when method 1 is used compared to method 2. In method 1, the data-quality estimates for neighbouring frames are strongly correlated because the full reflections used in the statistics are obtained by summing partials from consecutive frames. By contrast, in method 2 every frame produces estimates of full reflection intensities independently of the neighbouring frames. Therefore, the  $R$  factors per frame calculated after scaling with method 2 truly represent the data quality for individual frames.

11.5.7.4. Observed versus calculated partiality

The relationship between observed and calculated partialities (Fig. 11.5.7.6) deviates from the ideal line  $p_{\text{obs}} = p_{\text{calc}}$ , especially for the smaller calculated partialities where  $p_{\text{obs}} > p_{\text{calc}}$ . This suggests errors in the measurements of  $p_{\text{obs}}$  or the calculations of  $p_{\text{calc}}$ . The latter may be improved by a post refinement of the orientation matrix and crystal mosaicity (Rossmann *et al.*, 1979).

11.5.7.5. Anisotropic mosaicity

Refinement of the effective mosaicity can show both the anisotropic nature of the crystal (Fig. 11.5.7.7) as well as the impact of radiation damage. The effective mosaicity is the convolution of

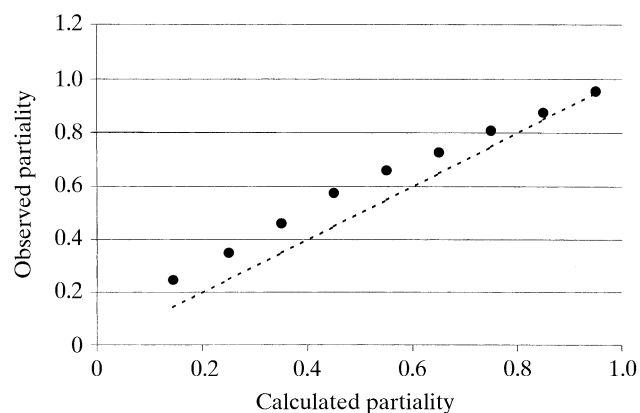


Fig. 11.5.7.6. The observed partialities plotted against calculated partialities for a  $\varphi$ X174 data set (Dokland *et al.*, 1997) processed by method 2. The observed partialities for individual partial reflections were averaged in bins of calculated partialities. The broken line represents the ideal relationship  $p_{\text{obs}} = p_{\text{calc}}$ .

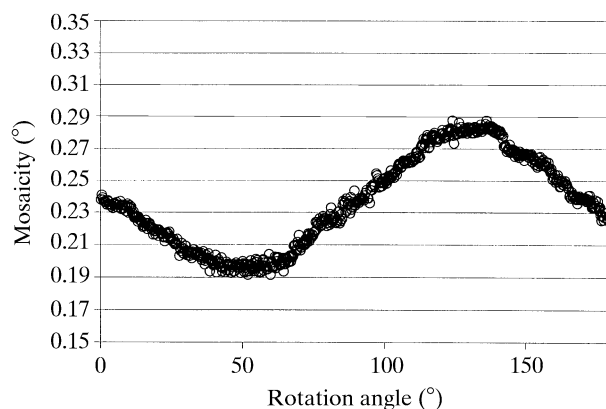


Fig. 11.5.7.7. Variation of (unconstrained) mosaicity for a monoclinic crystal of the bacterial virus alpha3 (Bernal *et al.*, 1998) showing the crystal anisotropy.

the mosaic spread of the crystal, the beam divergence and the wavelength divergence of the incident X-ray beam. Hence, X-ray diffraction data collected at a synchrotron-radiation source necessitate the differentiation of the effective mosaicity in the horizontal and vertical planes. A more general approach is the introduction of six parameters reflecting the anisotropic effective mosaicity.

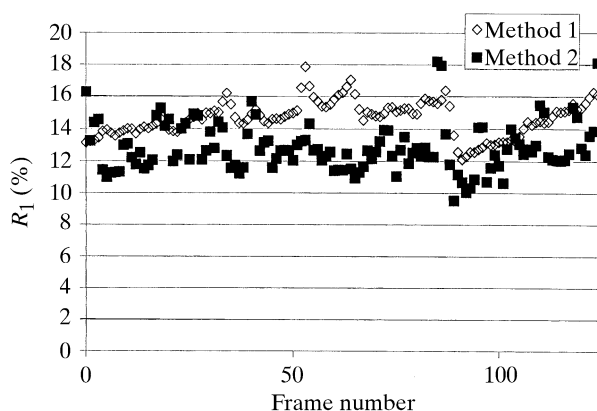


Fig. 11.5.7.5.  $R$  factor per frame as a function of frame number for a  $\varphi$ X174 data set (Dokland *et al.*, 1997).

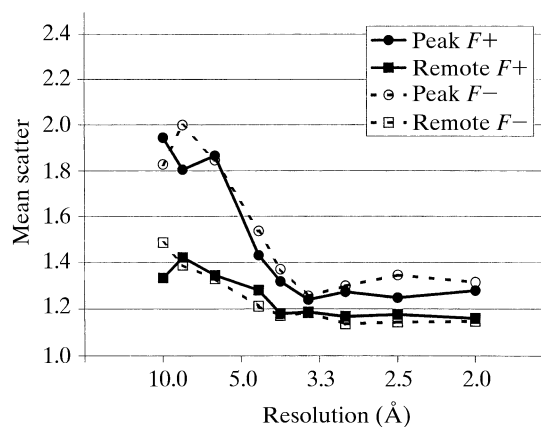


Fig. 11.5.7.8. Quality of anomalous-dispersion data for an SeMet derivative of dioxxygenase Rieske ferredoxin (Colbert & Bolin, 1999).